

# Ice Contamination of Meteosat/SEVIRI Implied by Intercalibration Against Metop/IASI

Tim J. Hewison, *Senior Member, IEEE*, and Johannes Müller

**Abstract**—The intercalibration of the infrared channels of the geostationary Meteosat/Spinning Enhanced Visible and InfraRed Imager (SEVIRI) satellite instruments shows that most channels are radiometrically consistent with those of Metop/IASI (Infrared Atmospheric Sounding Interferometer), which is used as a reference instrument. However, the 13.4- $\mu\text{m}$  channel shows a cold bias of  $\sim 1$  K in warm scenes, which changes with time. This is shown to be consistent with the contamination of SEVIRI by a layer of ice  $\sim 1$   $\mu\text{m}$  thick building up on the optics, which is believed to have condensed from water outgassed from the spacecraft. This ice modifies the spectral response functions and, hence, the weighting functions of the channels in stronger atmospheric absorption bands, thus introducing an apparent calibration error. Analysis of the radiometer's gain using an onboard black body source and a view of cold space confirms a loss consistent with transmission through a layer of comparable thickness, which also increases the radiometric noise—particularly for channels near the 12- $\mu\text{m}$  libration band of water ice. Intercalibration, such as the Global Space-based Inter-Calibration System Correction, offers an empirical method to correct this bias.

**Index Terms**—Calibration, decontamination, Earth-observing system, infrared (IR) image sensors, radiometers, satellites.

## I. INTRODUCTION

THE RADIOMETRIC calibration of broadband channels of satellite instruments can appear to be influenced by factors that modify the spectral response functions (SRFs). Most current infrared (IR) radiometers include calibration systems, typically using an onboard black body source and a view of cold space, which would appear to account for any such changes. However, a change in the instruments' SRF can modify the *weighting function*, which defines the vertical distribution of atmospheric emissions to which that channel is sensitive. This can introduce an apparent radiometric calibration error.

The intercalibration of the SEVIRI imagers on Meteosat-8 and Meteosat-9 with Metop-A/IASI revealed biases in the 13.4- $\mu\text{m}$  channels, which grow larger with time and change abruptly after decontamination procedures [1]. This supports the theory that the bias can be (at least partly) explained by a buildup of ice in the cold optics due to condensation of the outgassing material from the spacecraft. This paper considers this theory of contamination and attempts to model its impact

Manuscript received February 21, 2012; revised August 17, 2012; accepted September 30, 2012. Date of publication February 6, 2013; date of current version February 21, 2013.

The authors are with the European Organisation for the Exploitation of Meteorological Satellites (EUMETSAT), 64295 Darmstadt, Germany (e-mail: tim.hewison@eumetsat.int; johannes.mueller@eumetsat.int).

Color versions of one or more of the figures in this paper are available online at <http://ieeexplore.ieee.org>.

Digital Object Identifier 10.1109/TGRS.2012.2236335

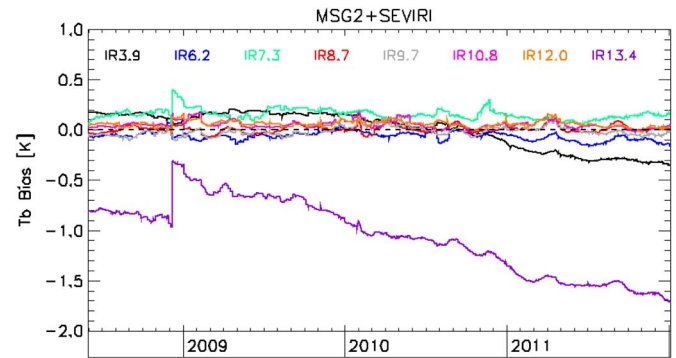


Fig. 1. Example time series plot showing the relative bias of the IR channels of Meteosat-9/SEVIRI (MSG2) wrt Metop-A/IASI, expressed as brightness temperature difference for standard radiance scenes (corresponding to a 1976 U.S. Standard Atmosphere with clear sky). A spacecraft decontamination in December 2008 reduced the bias of the 13.4- $\mu\text{m}$  channel, which subsequently continued to deteriorate.

on the calibration bias of SEVIRI's IR channels. These predictions are compared with observations—both in the form of intercalibration of SEVIRI with IASI—and by examination of SEVIRI's relative gain changes before and after decontamination procedures.

An example time series of the relative bias of the IR channels of Meteosat-9/SEVIRI with respect to Metop-A/IASI is shown in Fig. 1. These Global Space-based Inter-Calibration System (GSICS) *standard biases* correspond to radiance differences found with respect to the intercalibration reference in typical clear-sky conditions [1]. Most channels show small ( $< 0.4$  K) and stable biases during this period. However, the 13.4- $\mu\text{m}$  channel shows a negative bias, which slowly grows larger until a spacecraft decontamination event takes place in early December 2008, when the bias was reduced by about 0.7 K. It continues to degrade thereafter. The fact that the bias does not return to zero immediately after the decontamination suggests either that some contaminants remain after the decontamination or an inaccurate representation of the nominal SRF.

Variable biases of 1 K–2 K have also been observed in the 13.3- $\mu\text{m}$  channel of the Geostationary Operational Environmental Satellite, GOES-12 [1]. An analysis of the possible causes came to the conclusion that it was due to the failure of the imager anti-ice heater as well as erroneous characterization of the SRF during prelaunch testing [2].

## A. Decontamination Procedures

Condensation of a particle or chemical contamination on the cold optics of the SEVIRI affects the instrument's radiometric

TABLE I  
GAIN CHANGES MEASURED FOLLOWING  
METEOSAT-8 DECONTAMINATIONS

Date	2003-03	2003-08	2004-01	2005-01	2006-01	2008-01
Channel						
3.9 $\mu\text{m}$	+10%	n/a	+6%	+9%	+7%	+9%
6.2 $\mu\text{m}$	+24%	n/a	+7%	+12%	+9%	+13%
7.3 $\mu\text{m}$	+13%	n/a	+3%	+5%	+4%	+6%
8.7 $\mu\text{m}$	+10%	n/a	+4%	+6%	+5%	+6%
9.7 $\mu\text{m}$	+11%	n/a	+1%	+2%	+1%	+2%
10.8 $\mu\text{m}$	+52%	n/a	+12%	+19%	+14%	+18%
12.0 $\mu\text{m}$	+140%	+144%	+27%	+41%	+30%	+38%
13.4 $\mu\text{m}$	+101%	n/a	+20%	+30%	+22%	+33%

TABLE II  
GAIN CHANGES MEASURED FOLLOWING  
METEOSAT-9 DECONTAMINATIONS

Date	2006-02-	2006-06-	2006-12	2007-12	2008-12
Channel					
3.9 $\mu\text{m}$	+6%	+6%	+6%	+6%	+6%
6.2 $\mu\text{m}$	+21%	+8%	+6%	+10%	+7%
7.3 $\mu\text{m}$	+13%	+4%	+3%	+6%	+4%
8.7 $\mu\text{m}$	+8%	+6%	+4%	+6%	+3%
9.7 $\mu\text{m}$	+6%	+1%	+1%	+2%	+0%
10.8 $\mu\text{m}$	+44%	+22%	+14%	+23%	+16%
12.0 $\mu\text{m}$	+115%	+49%	+34%	+50%	+35%
13.4 $\mu\text{m}$	+66%	+27%	+23%	+30%	+23%

performance. Also, the passive cooling system is impacted by contamination, so that it loses its effectiveness and, in an extreme case, may not be able to maintain the instrument's operating temperature. Decontamination operations must be performed to ensure that the instrument remains within the acceptable mission limits. The process is relatively simple; however, it does take several days where nominal operations are not possible. Heaters are employed to warm the detector optics and the coolers, causing the contaminants to evaporate, after which the instrument is allowed to cool down back to 95 K. Several decontaminations have been performed on Meteosat-8 and Meteosat-9 since they were launched on August 28, 2002, and December 21, 2005, as listed in Tables I and II, respectively. These tables also list the mean changes in gain observed for the three detectors in each channel following each decontamination. The accumulation of contaminants on the cold surfaces slows down with time, as the abundance of such molecules decreases with mission time. After 2008, the impact of contaminations on the instrument or cooler performance was so far not considered large enough to justify a mission outage for a further decontamination campaign. However, this does not exclude potential decontaminations in the future.

TABLE III  
RADIOMETRIC NOISE LEVELS MEASURED BEFORE AND AFTER  
2008 DECONTAMINATIONS OF METEOSAT-8 AND METEOSAT-9

Date	Meteosat-8 2008-12		Meteosat-9 2008-12	
Channel	Before	After	Before	After
3.9 $\mu\text{m}$	0.11 K	0.11 K	0.10 K	0.10 K
6.2 $\mu\text{m}$	0.04 K	0.04 K	0.04 K	0.04 K
7.3 $\mu\text{m}$	0.06 K	0.06 K	0.05 K	0.05 K
8.7 $\mu\text{m}$	0.07 K	0.07 K	0.07 K	0.07 K
9.7 $\mu\text{m}$	0.11 K	0.11 K	0.11 K	0.11 K
10.8 $\mu\text{m}$	0.06 K	0.06 K	0.06 K	0.06 K
12.0 $\mu\text{m}$	0.13 K	0.11 K	0.12 K	0.10 K
13.4 $\mu\text{m}$	0.22 K	0.17 K	0.25 K	0.21 K

The long-wavelength channels are most affected by contamination, which peaks around the 12- $\mu\text{m}$  ice librational band. The gain increases observed following decontaminations are accompanied by a corresponding reduction in the radiometric noise, as shown in Table III. However, as the radiometric noise level is only recorded to two decimal places, there is greater uncertainty in their relative changes.

Similar decontamination procedures are conducted for the IASI [2], although the buildup of ice only increases its radiometric noise, without introducing an apparent calibration bias, because of its channels' high spectral resolution.

## II. THEORY

The basic hypothesis to be tested here is that the change in bias of the SEVIRI channels is due to a buildup of ice, which condenses on the surfaces of the cold optics after outgassing from other material on the satellite. This process has been known about since at least the time of Meteosat First Generation [4]. This material is most likely to be water ice [5]. However, since the rates of outgassing and condensation are unknown, it is not possible to estimate the ice thickness on purely theoretic grounds. Furthermore, it is not known exactly where in the instrument optics the ice is likely to condense, although in SEVIRI, the first surfaces to trap contaminants are the optical bandpass filters inside the cold IR optical bench [6]. The effect of contamination is difficult to assess because it depends on the optical surfaces that receive contaminants and their coatings' characteristics are not known. The contamination will affect both the gain of the associated channels and their SRFs, which will influence the radiometric noise and bias of the instrument's final calibrated radiances.

Differential absorption by this ice layer modifies the instrument's SRF. Although much of this is compensated for in the calibration processes, whereby the instrument's view of cold space and a hot black body are used to derive its gain and offset, any unidentified changes in the SRF could bias the observed scene radiances. This process is illustrated in Fig. 2, which

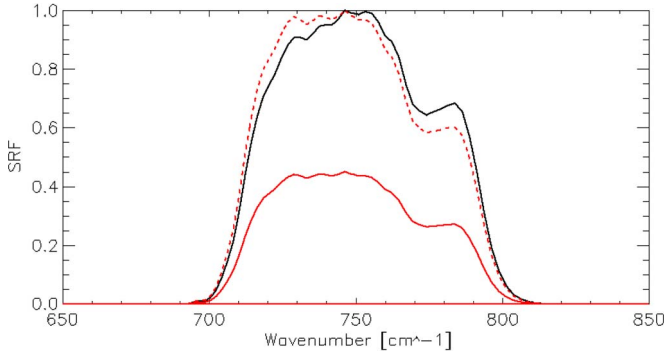


Fig. 2. SRFs of the Meteosat-9 13.4- $\mu\text{m}$  channel: The black solid line shows the nominal SRF based on prelaunch tests at 95 K, the red solid line shows the SRF convolved with the transmission spectrum of the ice layer 2  $\mu\text{m}$  thick, and the red dashed line shows the normalized SRF after the 2- $\mu\text{m}$  ice layer.

compares the nominal SRF of Meteosat-9's 13.4- $\mu\text{m}$  channel with that after convolving it with the transmission spectrum of a 2- $\mu\text{m}$ -thick layer of ice. The calibration process effectively normalizes the SRF, so it appears to be approximately shifted by 2  $\text{cm}^{-1}$  with respect to the original SRF. This illustrates why applying empirical shifts to the SRF can provide a good approximation to the channel's response to ice contamination.

The radiance  $L_i$  measured in channel  $i$  of an uncontaminated instrument, with SRF  $r_{i,\nu}$  viewing a scene with radiance spectrum  $L_\nu$ , is

$$L_i = \frac{\int L_\nu r_{i,\nu} d\nu}{\int r_{i,\nu} d\nu}. \quad (1)$$

Viewing the hot black body, with radiance  $B_\nu(T_H)$ , the uncontaminated instrument sees a radiance  $L_{i,H}$

$$L_{i,H} = \frac{\int B_\nu(T_H) r_{i,\nu} d\nu}{\int r_{i,\nu} d\nu}. \quad (2)$$

Viewing this scene when the SRF is convolved with an ice transmittance  $\tau_\nu$ , the radiance  $L'_{i,H}$  is

$$L'_{i,H} = \frac{\int B_\nu(T_H) r_{i,\nu} \tau_\nu d\nu}{\int r_{i,\nu} \tau_\nu d\nu}. \quad (3)$$

Assuming that the space-view radiances remain zero, the apparent gain of the instrument  $G_i = L'_{i,H}/L_{i,H}$  is applied to calculate the apparent radiance of a scene  $L'_i$

$$L'_i = \frac{\int L_\nu r_{i,\nu} \tau_\nu d\nu}{\int r_{i,\nu} \tau_\nu d\nu} \frac{L'_{i,H}}{L_{i,H}}. \quad (4)$$

#### A. Ice Transmittance Model

In this study, we use the composite model of ice optical constants compiled from various observations by Warren and Brandt [7]. Although these are strictly only valid at 266 K and are temperature dependent, no quantitative data were found for ice at temperatures close to those of SEVIRI's cold optics.

Fig. 3 shows the calculated transmittance spectra of various ice layers of thicknesses from 0.1 to 1.0  $\mu\text{m}$ , superimposed on the SRFs of the eight IR channels of Meteosat/SEVIRI.

Additionally, thin films of ice can introduce interference effects, which can modify its transmittance—particularly where

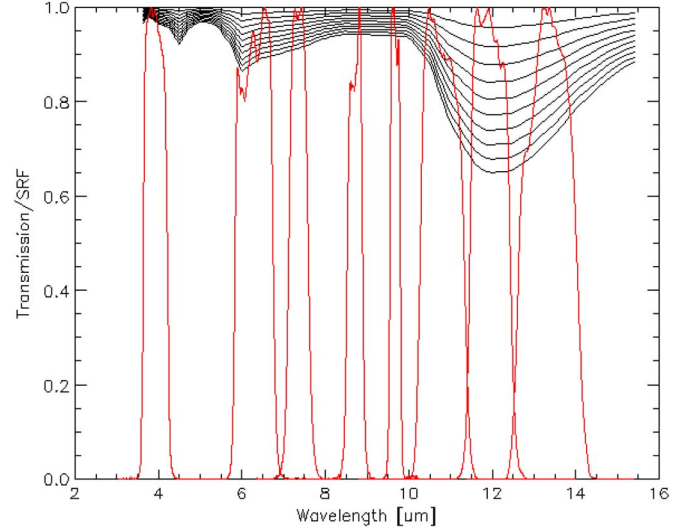


Fig. 3. (Black) Transmittance spectra of ice layers of different thicknesses: 0.1- to 1.0- $\mu\text{m}$  layers (the thickest layers have the lowest transmittance). (Red) SRFs of the Meteosat-8 IR channels.

its thickness approaches the wavelength of radiation. The effect of thin ice layers was analyzed for channels of Landsat/TM (Thematic Mapper) in the reflected solar band [8]. However, these have not been accounted for in this analysis, as the optical characteristics of the underlying surface are not known.

### III. PREDICTED AND OBSERVED GAIN AND BIAS CHANGES IN METEOSAT/SEVIRI

Modifications to an instrument's SRF will introduce an apparent bias, which will be scene dependent—varying not only with radiance but also with the scene spectra. Usually, the bias will be worse for clear-sky scenes with stronger spectral contrasts and smaller for overcast scenes, which are closer to the black body spectra.

To evaluate the difference between  $L'_i$  and  $L_i$ , a range of different radiance spectra  $L_\nu$  has been considered, and the calculation was repeated over the range of ice transmittance spectra  $\tau_{i,\nu}$ , given in Fig. 3. This was first performed for modeled radiance spectra corresponding to a U.S. Standard Atmosphere in clear-sky conditions, for which the GSICS *standard bias* [1] shown in Fig. 1 is evaluated. The calculation was also repeated with the addition of an optically thick layer of cloud with tops at 194 hPa, which produces brightness temperatures of  $\sim 216$  K–222 K. The radiative transfer simulation was performed using line-by-line radiative transfer model (LBLRTM) v11.1 with the for high-resolution transmission molecular absorption database (HITRAN) 2004 database with Atmospheric and Environmental Research (AER) v2.0 updates using the standard atmospheric profiles supplied with LBLRTM [9]. The resulting biases  $L'_i - L_i$  are expressed in terms of brightness temperatures in Fig. 4.

In clear skies, only the 13.4- $\mu\text{m}$  channel, which spans one side of an ice librational band, is predicted to have a significant sensitivity to ice contamination. This is because the ice modifies the SRF, and hence the weighting function, of this channel, which lies on the edge of an atmospheric  $\text{CO}_2$  absorption

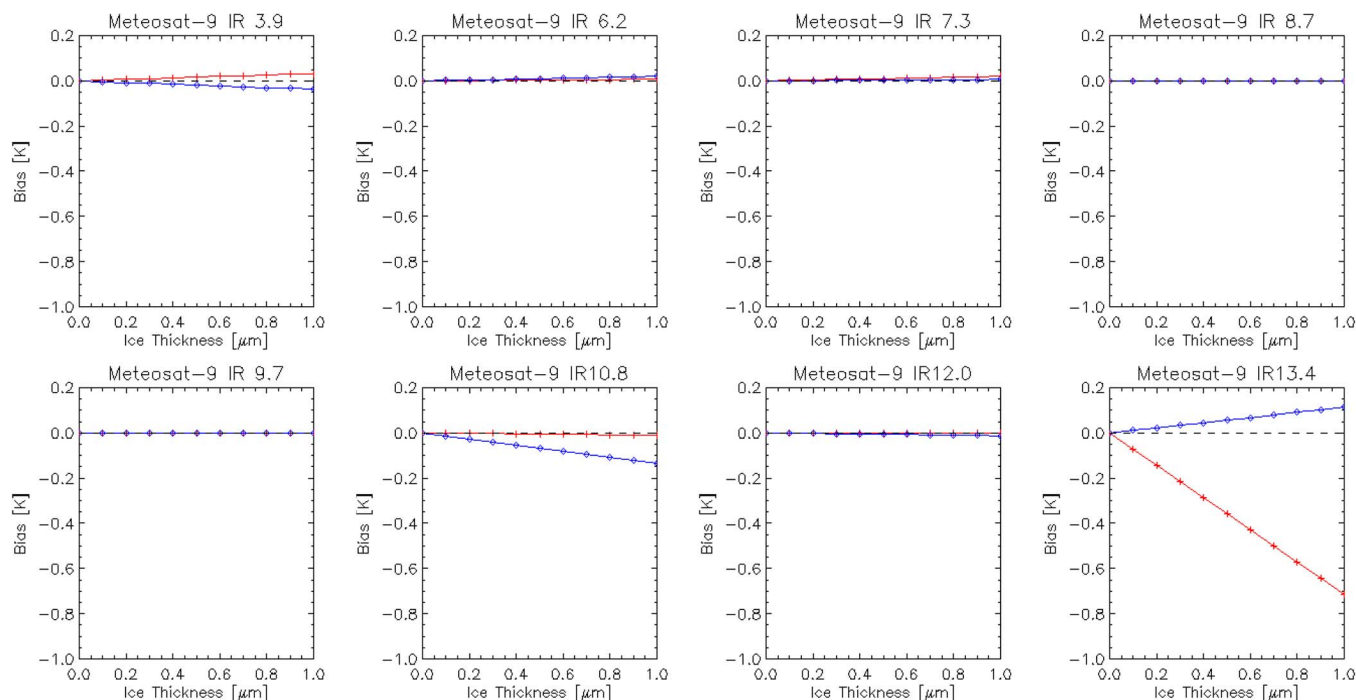


Fig. 4. Bias in brightness temperatures modeled by modifying Meteosat-9's SRFs by the transmittance of different thicknesses of ice. The solid lines show the predicted differences in brightness temperature compared with the uncontaminated instrument, accounting for calibration gain changes, based on calculation in U.S. Standard Atmosphere with (red line with crosses) clear skies and (blue line with diamonds) thick cloud with tops at 194 hPa.

band. The resulting  $\sim 0.7$ -K change in the *standard bias* of the  $13.4\text{-}\mu\text{m}$ -channel bias for an ice thickness of  $1\ \mu\text{m}$  is consistent with the changes observed in the intercalibration of Meteosat-9/SEVIRI during the 2008 decontamination. Since the decontamination, the bias in the  $13.4\text{-}\mu\text{m}$  channel has continued to increase at a rate of  $-0.4\ \text{K/year}$ .

The only other channel with a statistically significant trend in Fig. 1 is  $3.9\ \mu\text{m}$  ( $-0.1\ \text{K/year}$ ), which was not expected from the model results shown in Fig. 4. This may be due to thin-film effects, which can influence the transmittance of ice layers in this channel and cause nonmonotonic bias changes due to the buildup of ice layers with thickness on the order of wavelength. The longer wavelength of the  $13.4\text{-}\mu\text{m}$  channel means that thin-film effects will not become important until the thickness of the contamination layer approaches a fraction of its wavelength.

The intercalibration results after each decontamination procedure confirm that the biases in both these channels briefly return to values comparable to those found after the previous decontaminations but then continue to degrade. Meteosat-9 was launched later than Meteosat-8, so it is expected to have higher rates of outgassing and contamination, as witnessed by the higher rate of change of gains during decontaminations early in each spacecraft's life, shown in Tables I and II. However, the  $13.4\text{-}\mu\text{m}$  channel of both instruments showed jumps of  $\sim +0.7\ \text{K}$  during their most recent decontamination procedures in December and January 2008, respectively, despite both taking place approximately one year after the previous decontaminations.

Scenes with high cloud produce radiance spectra closer to those of a black body at the cloud top temperature ( $216\ \text{K}$ ). In these cases, a small positive brightness temperature bias at  $13.4\ \mu\text{m}$  is predicted, and a small negative bias is introduced

in the  $10.8\text{-}\mu\text{m}$  channel. However, because of the nonlinear nature of the Planck function, these biases are very small when converted into radiances. In practice, it would not be possible to detect such changes at low scene radiances because they are close to the standard uncertainty of the intercalibration at these scene radiances—and  $0.25\ \text{K}$  and  $0.08\ \text{K}$  for the  $10.8\text{-}$  and  $13.4\text{-}\mu\text{m}$  channels, respectively [10].

The calculations gave very similar results when repeated using Meteosat-8 SRFs and when using radiances modeled from tropical and midlatitude summer profiles. When cloud was added to the atmospheric profiles at low and middle levels, the predicted biases varied within the ranges shown in Fig. 4 for scenes with clear sky and high cloud.

Table II shows that a 35% change in gain in the  $12.0\text{-}\mu\text{m}$  channel was measured following the 2008 decontamination of Meteosat-9, which implies from Fig. 3 that the ice layer was  $\sim 1\ \mu\text{m}$  thick, similar to that required to produce a change in bias of  $\sim 0.7\ \text{K}$  for typical scene radiances, as shown in Fig. 4. Other channels are less sensitive to ice contamination, so there is more uncertainty in implying ice thickness from their gain changes. Nevertheless, the observed patterns of gain changes of the most recent decontaminations shown in Tables I and II are broadly consistent with ice thicknesses of  $\sim 1\ \mu\text{m}$ , and the relative changes between channels on other decontaminations follow the same pattern as the ice transmission spectra shown in Fig. 3.

Warren and Brandt estimated the uncertainty on the imaginary part of the refractive index of ice in their compilation as ranging from 2% to 20% over these wavelengths [7]. For weak to moderately absorbing ice layers, the uncertainty on the gain change and apparent calibration bias will be approximately linear with the uncertainty in the absorption coefficient. We

therefore assume that the standard uncertainty due to the refractive index model is  $\sim 25\%$ , accounting for the extrapolation of the model to low temperatures.

#### IV. CONCLUSION

The radiometric calibration of broadband channels of satellite instruments can appear to be influenced by factors that modify the SRFs. Although most current IR radiometers include calibration systems, typically using an onboard black body source and a view of cold space, a change in the instruments' SRF can modify the *weighting function*, which defines the vertical distribution of atmospheric emissions to which that channel is sensitive. If, as is usually the case, these changes are not accounted for by the users, they can appear as radiometric biases, which can be addressed empirically by applying corrections derived from intercalibration, such as the GSICS Corrections [1].

This analysis provides an example of how intercalibration can be a powerful tool in the diagnosis of the root causes of apparent radiometric errors in satellite instruments. Changes in the gain of Meteosat/SEVIRI's IR channels and the bias of its  $13.4\text{-}\mu\text{m}$  channel (by intercalibration with Metop/IASI) are shown to be consistent with contamination of its optics by the buildup of an ice layer  $\sim 1\ \mu\text{m}$  thick during the period in 2008 between decontaminations. The bias of this channel measured by the end of 2011 suggests that the ice may be twice this thick. However, the noise levels of the instrument remain within the required levels, so no further decontaminations have been conducted so far.

It may be possible to extend the simple model presented here to account for observed changes in the  $3.9\text{-}\mu\text{m}$  channel by including thin-film effects. Furthermore, a similar analysis could also be undertaken for other satellite instruments with broad SRFs, such as High-resolution Infra-Red Sounder—particularly those where intercalibration with respect to hyperspectral reference instruments is possible.

#### REFERENCES

- [1] T. J. Hewison, X. Wu, F. Yu, Y. Tahara, X. Hu, D. Kim, and M. Koenig, "GSICS inter-calibration of infrared channels of geostationary imagers using Metop/IASI," *IEEE Trans. Geosci. Remote Sens.*, vol. 51, no. 3, pp. 1160–1170, Mar. 2013.
- [2] F. Yu and X. Wu, "Correction for GOES imager spectral response function using GSICS II: Applications," *IEEE Trans. Geosci. Remote Sens.*, vol. 51, no. 3, pp. 1200–1214, Mar. 2013.

- [3] L. Buffet, E. Péquignot, D. Blumstein, R. Fjörtoft, V. Lonjou, B. Millet, and C. Larigauderie, "IASI instrument onboard Metop-A: Lessons learned after almost two years on orbit," in *Proc. ICSO Conf.*, Toulouse, France, Oct. 14–17, 2008.
- [4] J. Schmetz, L. van de Berg, and V. Gärtner, "Calibration of the Meteosat IR and WV channels for cloud studies and wind extraction," in *Proc. 10th Meteosat Sci. Users' Conf.*, Cascais, Portugal, Sep. 5–9, 1994, pp. 101–109.
- [5] D. Blumstein, CNES, personal communication, Mar. 12, 2008.
- [6] F. Pasternak, Astrium, personal communication, Jun. 5, 2007.
- [7] S. G. Warren and R. E. Brandt, "Optical constants of ice from the ultraviolet to the microwave: A revised compilation," *J. Geophys. Res.*, vol. 113, no. D14, p. D14220, Jul. 2008.
- [8] E. Micijevic and G. Chander, "Comparison of outgassing models for the Landsat Thematic Mapper sensors," in *Proc. SPIE*, 2007, vol. 6677G, p. 66770G.
- [9] S. A. Clough, M. W. Shephard, E. J. Mlawer, J. S. Delamere, M. J. Iacono, K. Cady-Pereira, S. Boukabara, and P. D. Brown, "Atmospheric radiative transfer modeling: A summary of the AER codes," *J. Quant. Spectrosc. Radiat. Transf.*, vol. 91, no. 2, pp. 233–244, Mar. 2005.
- [10] T. J. Hewison, "An evaluation of the uncertainty of the GSICS SEVIRI-IASI inter-calibration products," *IEEE Trans. Geosci. Remote Sens.*, vol. 51, no. 3, pp. 1171–1181, Mar. 2013.



**Tim J. Hewison** (M'96–SM'13) received the Ph.D. degree in meteorology from the University of Reading, Reading, U.K., in 2006, with a thesis on the use of ground-based microwave radiometers for atmospheric temperature and humidity profiling.

He is currently a Meteorological Scientist with the European Organisation for the Exploitation of Meteorological Satellites (EUMETSAT), Darmstadt, Germany, concentrating on the calibration of current, past, and future satellite instruments.

Dr. Hewison currently chairs the Research Working Group of the Global Space-based Inter-Calibration System.



**Johannes Müller** received the Dr. rer. nat. degree from the University of Cologne, Cologne, Germany, in 1991, with a thesis on the ground calibration of a satellite radiometer.

He worked for several research organizations as well as industry before joining the European Organisation for the Exploitation of Meteorological Satellites (EUMETSAT), Darmstadt, Germany, in 2005 as an Instrument Data Processing Engineer.